

Intramolecular Apical C–H···M Interactions in Square-Planar Nickel(II) Complexes with Dianionic Tridentate Ligands and 2-Phenylimidazole

Abhik Mukhopadhyay^[a] and Samudranil Pal^{*[a]}

Keywords: Nickel(II) complexes / Square-planar complexes / Apical C–H···Ni interactions / X-ray structures / Theoretical calculations

Two square-planar ternary nickel(II) complexes [Ni(bhac)(phim)] (**1**) and [Ni(ahac)(phim)] (**2**) with O,N,O-donor Schiff bases [acetylacetonone benzoylhydrazone (H₂bhac) and acetylacetonone acetylhydrazone (H₂ahac)] and sp² N-donor 2-phenylimidazole (phim) as the ancillary ligand have been synthesised and characterised by analytical, spectroscopic, magnetic and electrochemical methods. The solid-state structures of both complexes have been determined by X-ray crystallography. The asymmetric unit of **1** contains a single complex molecule while that of **2** contains four complex molecules with different conformations. The molecular structures of both complexes reveal that one of the two *ortho* C–H groups of the pendant phenyl ring of the phim ligand is very close to the metal centre at the apical site indicating the presence of an intramolecular C–H···Ni interaction. In the structures of **1** and **2**, the shape of the C–H···Ni interaction is determined by the twisting of the phim ligand and the extent of orthogo-

nality between the planes containing the chelate rings formed by the tridentate ligand and the imidazole ring. A survey of the reported X-ray structures of similar d⁸ metal ion complexes containing intramolecular C–H···M interactions has been performed for comparison with the structural features of **1** and **2**. The optimised molecular structures of **1** and **2** generated by calculations based on the density functional method are compared with the experimental structures. Calculations also reveal that the four molecules present in the asymmetric unit of **2** are very close in energy. Theoretical studies and the down-field shift of the proton resonance on cooling in the NMR spectra suggest three-centre four-electron hydrogen-bond character of the observed apical C–H···Ni interaction in **1** and **2**.

(© Wiley-VCH Verlag GmbH & Co. KGaA, 69451 Weinheim, Germany, 2006)

Introduction

The long standing interest in the interaction of transition metal ions with proximate C–H fragments is primarily due to the C–H activation processes involved in many catalytic reactions. Such interactions have been scrutinised intensively for a better understanding of their structural and bonding features.^[1–12] The C–H···M interaction in coordinatively unsaturated and electron-deficient (16-electron) species is called an agostic interaction or agostic bond where the filled C–H σ orbital interacts with an empty metal orbital. In these agostic interactions, generally the C–H fragment is side-on to the metal ion. This T-shape of the agostic C–H···M interaction facilitates the involvement of the filled metal $d\pi$ orbital and the empty C–H σ^* orbital in back bonding. However, the nature of the apical C–H···M interactions in square-planar 16-electron complexes of d⁸ metal ions is not very clear.^[9–12] In such species, these interactions can be agostic bond (three-centre two-electron) as well as non-classical hydrogen bond (three-centre four-electron)

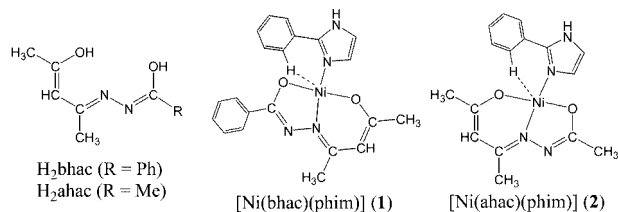
in character because of the availability of the empty orbital as well as the lone pair of electrons on the metal ion. Such apical C–H···M interactions in square-planar d⁸ systems have been described as weakly agostic bonds, non-classical hydrogen bonds and also as repulsive because of the filled metal d_{z^2} and C–H σ -orbitals.^[2,12–14] Compared with the agostic interaction the nonclassical hydrogen bond is not common in metal complexes. For a metal centre to participate as the proton acceptor in a hydrogen bond, it is essential for it to be electron rich. Examples of such complexes occur mostly with d⁸ and d¹⁰ metal centres. It has been demonstrated that such hydrogen bonds can facilitate the oxidative addition of H–X to a metal centre.^[15]

Herein we report two square-planar nickel(II) complexes with the tridentate Schiff bases H₂bhac and H₂ahac and the monodentate 2-phenylimidazole as the ancillary ligand. The deprotonated Schiff bases (bhac²⁻ and ahac²⁻) satisfy the +2 charge on the metal ion and three coordination sites. The sp² N atom of the neutral 2-phenylimidazole (phim) occupies the fourth coordination site and completes the N₂O₂ square plane around the metal ion. The ancillary ligand 2-phenylimidazole has been specifically chosen so that one of the two *ortho* C–H groups of the phenyl ring can be in close proximity with the metal ion at the apical site. The complexes, [Ni(bhac)(phim)] (**1**) and [Ni(ahac)(phim)] (**2**),

[a] School of Chemistry, University of Hyderabad, Hyderabad 500 046, India
Fax: +91-40-2301-2460
E-mail: spsc@uohyd.ernet.in

Supporting information for this article is available on the WWW under <http://www.eurjic.org> or from the author.

have been characterised by analytical, magnetic, spectroscopic and electrochemical measurements. The X-ray structures of **1** and **2** indeed reveal the presence of an apical C–H...M interaction in both complex molecules. We have examined the reported structures of the square-planar d⁸ systems with similar intramolecular C–H...M interactions available in the Cambridge Structural Database for a comparison with the structural features of **1** and **2**. Calculations based on density functional methods have been performed to understand the molecular conformations and the nature of the C–H...Ni interaction observed in the X-ray structures of **1** and **2**. Variable temperature NMR spectroscopic measurements have been carried out to probe the nature of this interaction in solution.



Results and Discussion

Synthesis and Some Properties

The reactions of 1 equiv. each of $\text{Ni}(\text{O}_2\text{CCH}_3)_2 \cdot 4\text{H}_2\text{O}$, the Schiff bases (H_2bhac and H_2ahac) and 2-phenylimidazole in boiling methanol afford the dark brown complexes in moderate to good yields. Elemental analysis data are consistent with the molecular formula $[\text{Ni}(\text{bhac})(\text{phim})]$ (**1**) and $[\text{Ni}(\text{ahac})(\text{phim})]$ (**2**). Both **1** and **2** are electrically nonconducting in methanol solutions. The complexes are diamagnetic and NMR spectroscopically active. Thus in each complex, the nickel ion is in the +2 oxidation state and the coordination geometry around the metal centre is square planar.

The infrared spectra of **1** and **2** do not display any band assignable to the amide or secondary amine N–H stretch.^[16] Several sharp weak bands observed in the range 2900–3150 cm^{-1} are likely to be due to the C–H stretches. The absence of any band for the N–H group of the ancillary ligand phim is consistent with its involvement in strong intermolecular hydrogen bonding (vide infra). Free H_2bhac and H_2ahac display the amide C=O stretch^[17] near $\approx 1675 \text{ cm}^{-1}$. The absence of any such band in the spectra of **1** and **2** indicates complete deprotonation of the Schiff bases in the complexes. Thus in both complexes, the dianionic tridentate ligands (bhac^{2-} and ahac^{2-}) act as the enolate-O, the imine-N and the deprotonated amide-O donor. A strong band observed near 1590 cm^{-1} might involve the C=N stretches.^[18,19]

The electronic spectra were collected using methanol solutions of the complexes. Both complexes display several absorptions. For **1** the absorption bands are in the range 565–234 nm and those for **2** are within 425–235 nm. The density functional calculations show that in both **1** and **2**

the lowest unoccupied molecular orbital (LUMO) is primarily localised on the ancillary ligand phim and the highest occupied molecular orbital (HOMO) is composed of d and p orbitals of the metal and coordinated O atoms, respectively. The spectra of the free Schiff bases and 2-phenylimidazole in methanol solutions display a single absorption in the range 250–215 nm. Thus the absorptions observed for **1** and **2** are possibly due to the metal-to-ligand and inter- or intra-ligand charge-transfer transitions.

Electron transfer properties of **1** and **2** have been investigated by cyclic voltammetry using acetonitrile solutions of the complexes. Both **1** and **2** display an irreversible oxidation response at 0.69 and 0.71 V, respectively. The current height of this response is comparable with known one-electron redox processes under identical conditions.^[19,20] No such response is observed for the deprotonated Schiff bases and 2-phenylimidazole under the same conditions. The iron(III) and copper(II) complexes with bhac^{2-} show metal-centred oxidation responses in the potential range 0.4–0.8 V.^[21–23] Therefore, the oxidation responses observed for **1** and **2** are assigned to a $\text{Ni}^{\text{II}} \rightarrow \text{Ni}^{\text{III}}$ process. The nature of the HOMO in both complexes also supports this assignment. The irreversible nature of the response suggests that in each case the corresponding oxidised species is unstable on the cyclic voltammetry time scale.

Description of X-ray Structures and C–H...Ni Interactions

The molecular structures of **1** and **2** are depicted in Figure 1. Bond parameters associated with the metal ions are listed in Table 1. The asymmetric unit of **1** contains one complex molecule while that of **2** contains four complex molecules. In each molecule, the enolate-O, the imine-N and the deprotonated amide-O donor tridentate ligand and the imine-N donor monodentate phim form a N_2O_2 square plane around the metal centre. There is no deviation of the metal centre from the N_2O_2 square plane. The Ni–O(enolate), Ni–N(imine), Ni–O(amide) and Ni–N(imidazole) bond lengths are comparable with those observed in nickel-

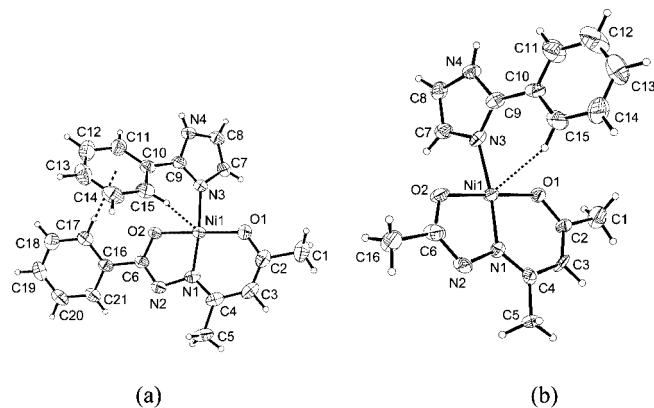


Figure 1. Molecular structures of (a) $[\text{Ni}(\text{bhac})(\text{phim})]$ (**1**) and (b) $[\text{Ni}(\text{ahac})(\text{phim})]$ (**2**) with the atom labelling scheme. All non-hydrogen atoms are represented by their 40% probability thermal ellipsoids.

(II) complexes having the same coordinating atoms.^[24–26] The average N–C and C–O bond lengths in the –N=C(O[–])– fragments^[21–26] and the C–C and C–O bond lengths in the –C=C(O[–])– fragments^[21–24] are consistent with the enolate form of both amide and acetylacetonate moieties of the tridentate ligands.

Table 1. Selected bond lengths [Å] and bond angles [°] for **1** and **2**.

| [Ni(bhac)(phim)] (1) | | | |
|-------------------------------|------------|-------------------|------------|
| Ni(1)–O(1) | 1.8195(17) | Ni(1)–O(2) | 1.8443(16) |
| Ni(1)–N(1) | 1.8269(18) | Ni(1)–N(3) | 1.9136(18) |
| O(1)–Ni(1)–O(2) | 175.76(7) | O(1)–Ni(1)–N(1) | 96.15(7) |
| O(1)–Ni(1)–N(3) | 89.07(7) | O(2)–Ni(1)–N(1) | 84.13(7) |
| O(2)–Ni(1)–N(3) | 91.08(7) | N(1)–Ni(1)–N(3) | 172.37(8) |
| [Ni(ahac)(phim)] (2) | | | |
| Molecule 1 | | | |
| Ni(1)–O(1) | 1.829(5) | Ni(1)–O(2) | 1.851(5) |
| Ni(1)–N(1) | 1.826(6) | Ni(1)–N(3) | 1.923(6) |
| O(1)–Ni(1)–O(2) | 178.3(2) | O(1)–Ni(1)–N(1) | 95.6(3) |
| O(1)–Ni(1)–N(3) | 91.4(2) | O(2)–Ni(1)–N(1) | 84.0(2) |
| O(2)–Ni(1)–N(3) | 89.0(2) | N(1)–Ni(1)–N(3) | 173.0(3) |
| Molecule 2 | | | |
| Ni(2)–O(3) | 1.818(5) | Ni(2)–O(4) | 1.852(5) |
| Ni(2)–N(5) | 1.821(7) | Ni(2)–N(7) | 1.909(6) |
| O(3)–Ni(2)–O(4) | 177.8(2) | O(3)–Ni(2)–N(5) | 96.0(3) |
| O(3)–Ni(2)–N(7) | 90.3(3) | O(4)–Ni(2)–N(5) | 83.8(3) |
| O(4)–Ni(2)–N(7) | 89.8(3) | N(5)–Ni(2)–N(7) | 173.6(3) |
| Molecule 3 | | | |
| Ni(3)–O(5) | 1.820(5) | Ni(3)–O(6) | 1.855(5) |
| Ni(3)–N(9) | 1.820(6) | Ni(3)–N(11) | 1.918(6) |
| O(5)–Ni(3)–O(6) | 178.3(3) | O(5)–Ni(3)–N(9) | 95.6(3) |
| O(5)–Ni(3)–N(11) | 89.4(3) | O(6)–Ni(3)–N(9) | 84.3(3) |
| O(6)–Ni(3)–N(11) | 90.5(3) | N(9)–Ni(3)–N(11) | 174.2(3) |
| Molecule 4 | | | |
| Ni(4)–O(7) | 1.832(6) | Ni(4)–O(8) | 1.853(5) |
| Ni(4)–N(13) | 1.838(6) | Ni(4)–N(15) | 1.928(7) |
| O(7)–Ni(4)–O(8) | 179.6(3) | O(7)–Ni(4)–N(13) | 96.0(3) |
| O(7)–Ni(4)–N(15) | 89.4(3) | O(8)–Ni(4)–N(13) | 83.7(3) |
| O(8)–Ni(4)–N(15) | 91.0(3) | N(13)–Ni(4)–N(15) | 173.5(3) |

In **1**, the tridentate ligand bhac^{2–} is not planar because of the twisting of the phenyl ring plane along the C6–C16 bond (Figure 1). The dihedral angle between the phenyl ring plane and the plane constituted by the rest of the atoms in bhac^{2–} is 25.56(8)°. It is also interesting to note that one of the two *ortho* C–H groups of the phenyl ring of bhac^{2–} is involved in a C–H··· π interaction with the phenyl ring of the ancillary ligand phim (Figure 1). The H···Cg distance and the C–H···Cg angle are 2.962 Å and 153°, respectively. Possibly this C–H··· π interaction is primarily responsible for the twisting of the phenyl ring plane of bhac^{2–}

along the C6–C16 bond. The O1–Ni1–N3–C9 torsion angle (θ) is 48.9° (Table 2). Thus the chelate forming fragment (O1,O2,N1,N2,C1–C6) of bhac^{2–} and the metal coordinated imidazole ring plane are not orthogonal (Figure 1). The phim moiety is not planar because of the twisting of the imidazole ring plane and the phenyl ring plane along the C9–C10 bond (Figure 1). The extent of twisting (ψ) is measured by taking the average of the N3–C9–C10–C15 and N4–C9–C10–C11 torsion angles. The value of ψ is calculated as 35.8°. As a result an *ortho* C–H group of the phim phenyl ring is close to the metal centre at the apical site (Figure 1). The Ni···H and Ni···C distances and the Ni···H–C angle are 2.79(2), 3.321(3) Å and 116.8(2)°, respectively (Table 2).

The bond lengths and bond angles of the four molecules present in the asymmetric unit of **2** are very similar (Table 1). However, the orthogonality (θ) between the chelate forming fragment of ahac^{2–} and the metal coordinated imidazole ring plane and the twisting of phim (ψ) differ significantly. The θ and ψ values are in the ranges 72.9–91.6° and 1.6–21.6°, respectively (Table 2). Most importantly in two molecules the orientation of the phim phenyl ring with respect to the {Ni(ahac)} plane is on one side and in the other two molecules it is on the other side (Figure 2). As in **1**, one of the two *ortho* C–H groups of the phim phenyl ring is close to the metal centre at the apical site in each of the four molecules. The Ni···H and Ni···C distances and the C–H···Ni angles are within 2.42–2.69 Å, 3.20–3.36 Å, and 130.1–142.2°, respectively (Table 2).

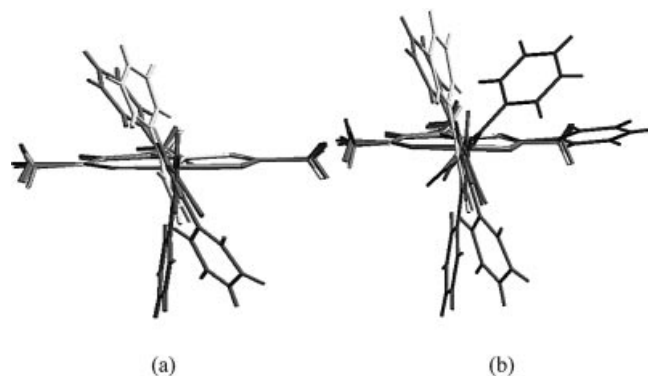


Figure 2. Overlay diagrams of (a) the four molecules present in the asymmetric unit of [Ni(ahac)(phim)] (**2**), and (b) the molecule of [Ni(bhac)(phim)] (**1**) and the four molecules of [Ni(ahac)(phim)] (**2**).

Table 2. Structural parameters related to C–H···Ni interactions and molecular conformations of **1** and **2**.

| Parameters | [Ni(bhac)(phim)] (1) | | [Ni(ahac)(phim)] (2) | | | | Calculated |
|-----------------------------|-------------------------------|------------|-------------------------------|------------|------------|------------|------------|
| | Experimental | Calculated | Experimental | Molecule 1 | Molecule 2 | Molecule 3 | |
| Ni···H distance [Å] | 2.79(2) | 2.48 | 2.54 | 2.42 | 2.47 | 2.69 | 2.51 |
| Ni···C distance [Å] | 3.321(3) | 3.26 | 3.288(9) | 3.207(9) | 3.236(12) | 3.364(11) | 3.23 |
| C–H···Ni angle [°] | 116.8(2) | 125 | 137.7 | 142.2 | 139.3 | 130.1 | 127 |
| ψ ^[a] [°] | 35.8 | 28 | 12.9 | 1.6 | 11.3 | 21.6 | 27 |
| θ ^[b] [°] | 48.9 | 56 | 73.1 | 91.6 | 76.4 | 72.9 | 58 |

[a] Average of N3–C9–C10–C15 and N4–C9–C10–C11 torsion angles. [b] O1–Ni–N3–C9 torsion angle.

The following trends are very clear from the above observations on the molecular structures of **1** and **2**. In **1**, only one complex molecule is present in the asymmetric unit and both the phenyl ring and the imidazole ring planes of phim are tilted toward the phenyl ring of the benzoyl fragment of bhac²⁻ (Figure 1). In spite of being weak in nature we believe that the intramolecular C–H \cdots π interaction plays a major role in restricting the phim moiety from taking random orientations and a single conformation of it is stabilized in **1**. Because of the replacement of the phenyl group of bhac²⁻ by a methyl group in ahac²⁻ the C–H \cdots π interaction of the type observed in **1** is not possible in **2**. Complex **2** crystallises with four molecules in the asymmetric unit and the phim moieties are randomly oriented on both sides of the plane containing the {Ni(ahac)} moiety. Thus the lack of the C–H \cdots π interaction facilitates free rotation of phim about the Ni–N(imidazole) bond. In addition, the imidazole plane in **2** is closer to the orthogonal arrangement with the plane containing the two chelate rings ($\theta = 72.9$ – 91.6°) compared with that in **1** ($\theta = 48.9^\circ$). This difference is also likely to be because of the C–H \cdots π interaction in **1**. The internal twisting of phim in **1** ($\psi = 35.8^\circ$) is significantly larger than that in **2** ($\psi = 1.6$ – 21.6°). Possibly this difference is also partly due to the intramolecular C–H \cdots π interaction in **1**. Despite the differences in the θ and ψ values one of the two *ortho* C–H groups of the phim phenyl ring is near to the apical position of the metal ion in all the structures. In this context, it may be noted that the crystal structure of the protonated 2-phenylimidazole (Hphim⁺) is known.^[27] Here the ψ value is 22.32° . Thus in all probability significantly different twisting of phim in **1** and **2** compared with that in Hphim⁺ is due to the intramolecular C–H \cdots π and C–H \cdots Ni interactions observed in the present complex molecules.

A close scrutiny of the structural parameters (Table 2) related to the C–H \cdots Ni interactions and the molecular conformations of **1** and **2** reveals the following. The longer the Ni \cdots H distance the shorter the C–H \cdots Ni angle. There is a satisfactory linear correlation between the Ni \cdots H distance and the C–H \cdots Ni angle (Figure S1, Supporting Information). The values of the Ni \cdots H distances and the corresponding C–H \cdots Ni angles strongly depend on the molecular conformations. In general, the Ni \cdots H distance increases and the C–H \cdots Ni angle decreases with the increase of the twisting (ψ) of phim and the decrease of the orthogonality (θ) between the imidazole ring plane and the plane containing the two chelate forming fragments of the tridentate ligands (Table 2). The Ni \cdots H distance is linearly related to the ψ values as well as θ values with opposite slopes (Figure S1). Thus a large twist of the phim ligand forces a T-shape of the C–H \cdots Ni interaction with an increase in the Ni \cdots H distance, while a small twist of the phim ligand makes the C–H \cdots Ni interaction more linear with a decrease in the Ni \cdots H distance. It is clear from the above facts that the geometrical arrangement of the C–H \cdots Ni interaction largely depends on the twist of the phim ligand in **1** and **2**. A detailed theoretical study reported previously has supported the idea that the axial M \cdots H interactions in d⁸ metal

ion complexes are mainly repulsive in nature.^[10] But a minor attractive contribution to the C–H \cdots M interaction can not be ruled out in the present complexes. The Ni \cdots H distances in both complexes and shorter Ni \cdots H distances in **2** compared with that in **1**, unaided and unhindered by any geometrical constraint in the former, substantiate this idea.

Intermolecular Hydrogen Bonds and Self-Assembly of **1** and **2**

Both complex molecules contain the imidazole N–H group and metal coordinated O atoms, which are conventional hydrogen-bond donors and acceptors, respectively. In the crystal lattice, the molecules of each of the two complexes are involved in intermolecular N–H \cdots O hydrogen bonding interactions involving the imidazole N–H groups and the metal coordinated amide O atoms of the tridentate ligands. In the case of **1**, the N \cdots O distance and the N–H \cdots O angle are 2.856(3) Å and 160(2)°, respectively. There are some variations in the geometrical parameters related to the N–H \cdots O interactions for the four molecules present in the asymmetric unit of **2**. The N \cdots O distances are in the range 2.788(8)–2.846(9) Å and the N–H \cdots O angles are within 148–163°. In each case, self-assembly of the complex molecules through these intermolecular N–H \cdots O hydrogen bonds leads to a one-dimensional supramolecular structure in the crystal lattice (Figure 3).

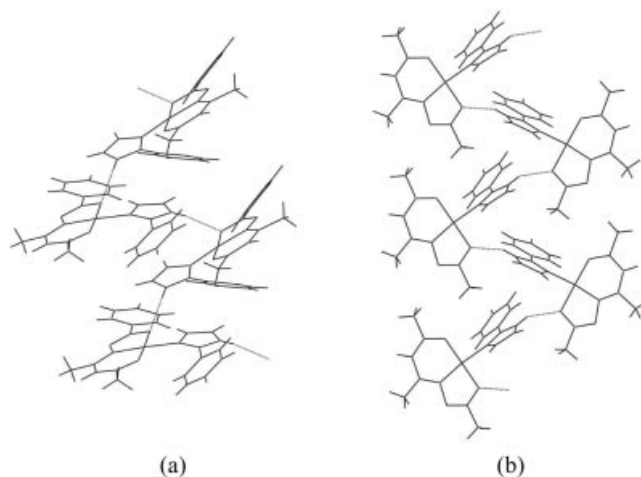


Figure 3. One-dimensional ordering of (a) [Ni(bhac)(phim)] (**1**) and (b) [Ni(ahac)(phim)] (**2**) through intermolecular N–H \cdots O hydrogen bonds.

Survey of the d⁸ Metal Ion Complexes with Intramolecular C–H \cdots M Interactions

The molecular structures of **1** and **2** show that the Ni \cdots H distance, the C–H \cdots Ni angle and hence the shape (T or linear) of the C–H \cdots Ni interaction largely depend on the twisting (ψ) of 2-phenylimidazole (vide supra). The Ni \cdots H distance is linearly related with ψ and the C–H \cdots Ni angle (Figure S1). To verify whether the trends observed for **1** and **2** are general or not we have performed a Cambridge Structural Database (version 5.26) search for d⁸ metal ion com-

plexes having intramolecular C–H···M interactions. The search was based on the following criteria: (i) the metal ion is always coordinated to a N atom that is bonded to the atom X (elements of groups 14–16), (ii) X is connected to an unsubstituted/substituted phenyl ring by a single bond, (iii) the phenyl ring *ortho* C–H at the δ position is involved in the C–H···M interaction, (iv) the M···H separation is in the range 2.0–3.0 Å, (v) the N_{α} – X_{β} – C_{γ} angle is within 110–140°, (vi) the N_{α} – X_{β} – C_{γ} – C_{δ} torsion angle (ψ) is in the range 0–180° and (vii) structures with *R* factors > 10 are excluded.

The number of hits obtained was 44. Selected structural parameters of these 44 X-ray structures are listed in Table 3.

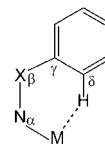


Table 3. Structural data for the intramolecular C–H···M interaction in d^8 metal ion complexes.

| Refcode | M ^{II} | M···H dist. [Å] | C–H···M angle [°] | ψ [°] |
|----------|------------------|-----------------|-------------------|------------|
| COPGET | Ni ^{II} | 2.668 | 125.102 | 33.573 |
| DAWGUD | Ni ^{II} | 2.885 | 102.297 | 85.365 |
| ERURAK | Ni ^{II} | 2.885 | 94.712 | 87.400 |
| ERUREO | Ni ^{II} | 2.733 | 109.016 | 77.854 |
| FAKVIW | Ni ^{II} | 2.894 | 93.133 | 85.339 |
| GIGVEX10 | Ni ^{II} | 2.859 | 107.358 | 88.293 |
| IFAFIE | Ni ^{II} | 2.476 | 136.801 | 12.763 |
| KIYQUE | Ni ^{II} | 2.792 | 129.004 | 36.500 |
| KOHHAQ | Ni ^{II} | 2.810 | 128.477 | 55.681 |
| LOKZOA | Ni ^{II} | 2.919 | 101.781 | 88.010 |
| LUQJOW | Ni ^{II} | 2.833 | 90.816 | 86.319 |
| MIYQEQ | Ni ^{II} | 2.607, | 123.717, | 31.403, |
| | | 2.972 | 99.198 | 31.403 |
| NOKVOY | Ni ^{II} | 2.663 | 105.555 | 77.495 |
| QOZROM | Ni ^{II} | 2.353 | 140.411 | 14.618 |
| RORHUB | Ni ^{II} | 2.869 | 90.055 | 86.797 |
| SENHIC | Ni ^{II} | 2.874 | 114.987 | 75.856 |
| SOSVAX | Ni ^{II} | 2.786 | 90.748 | 37.947 |
| SOSVAX10 | Ni ^{II} | 2.786 | 90.750 | 37.948 |
| TISPEQ | Ni ^{II} | 2.844 | 111.106 | 77.368 |
| TISPIU | Ni ^{II} | 2.967 | 108.425 | 82.605 |
| VETPEP | Ni ^{II} | 2.979 | 97.906 | 90.369 |
| BABDIS | Pd ^{II} | 2.703 | 119.125 | 73.137 |
| BECGEV | Pd ^{II} | 2.949 | 117.971 | 70.944 |
| CAPVOE | Pd ^{II} | 2.585, | 125.092, | 15.776, |
| | | 2.732 | 115.835 | 1.934 |
| DAGGUN | Pd ^{II} | 2.946 | 112.824 | 15.596 |
| DUHYUA | Pd ^{II} | 2.783 | 102.092 | 43.831 |
| DUNWAK | Pd ^{II} | 2.944 | 99.833 | 45.921 |
| EFODEI | Pd ^{II} | 2.884 | 107.519 | 31.598 |
| HAPNIV | Pd ^{II} | 2.926 | 115.268 | 16.080 |
| HOZNUF | Pd ^{II} | 2.880, | 100.278, | 85.396, |
| | | 2.836 | 96.338 | 84.995 |
| JEDDIF | Pd ^{II} | 2.865 | 102.679 | 79.360 |
| KIMXOT | Pd ^{II} | 2.871 | 132.141 | 54.848 |
| LANBIL | Pd ^{II} | 2.968 | 108.260 | 79.553 |
| LIJHUH | Pd ^{II} | 2.946 | 106.715 | 88.674 |
| NINMAY | Pd ^{II} | 2.933, | 119.920, | 69.726, |
| | | 2.744 | 128.876 | 62.872 |
| NOKGUP | Pd ^{II} | 2.823 | 108.391 | 57.224 |
| SUGWEW | Pd ^{II} | 2.596 | 133.835 | 54.013 |
| TURKIA | Pd ^{II} | 2.679 | 122.982 | 68.115 |
| UGIKOK | Pd ^{II} | 2.983, | 110.515, | 14.014, |
| | | 2.953, | 114.306, | 10.811, |
| | | 2.843 | 122.513 | 3.029 |
| XODPEL | Pd ^{II} | 2.815 | 107.154 | 48.564 |
| YIYHIX | Pd ^{II} | 2.833 | 117.149 | 72.866 |
| ZODQOY | Pd ^{II} | 2.868 | 101.858 | 86.739 |
| HAPZPT10 | Pt ^{II} | 2.966 | 90.958 | 68.292 |
| HIXJUT | Pt ^{II} | 2.854, | 125.650, | 12.480, |
| | | 2.976 | 131.625 | 33.951 |

In the structures collected in Table 3, the mean M···H distance increases in the order Ni^{II} < Pd^{II} < Pt^{II}. These values are 2.795, 2.841 and 2.932 Å for Ni^{II}, Pd^{II} and Pt^{II}, respectively. This order is expected as the van der Waals radius increases in the order Ni^{II} < Pd^{II} < Pt^{II}.^[10] In contrast to the structures of **1** and **2**, there is no readily apparent relationship between the M···H distance and the N_{α} – X_{β} – C_{γ} – C_{δ} torsion angle (ψ). However, the scattergram of ψ against the M···H distance (Figure 4a) shows the prevailing trend of long M···H distances for large ψ values. On the other hand, the M···H distance generally increases with the decrease of the C–H···M angle (Figure 4b) as observed for **1** and **2**. In other words, the C–H···M interaction becomes more T-shaped with the increase of the M···H distance.

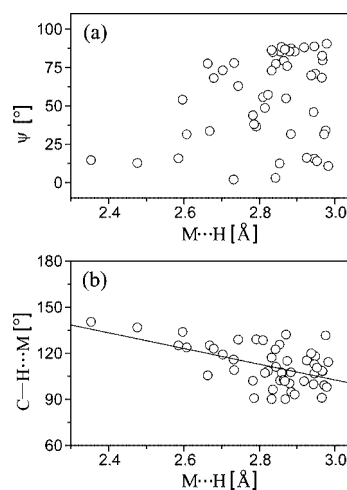


Figure 4. Scattergrams of (a) ψ (see text for definition) vs. M···H distance and (b) C–H···M angle vs. M···H distance. The straight line in (b) represents the least-squares fit.

Computational Results

Calculations based on density functional methods have been performed for structural optimisations of **1** and **2**. Each of the two complex molecules was computed as a complete system to consider all steric and electronic factors of the tridentate ligand (bhac²⁻ or ahac²⁻) and of the monodentate ancillary ligand 2-phenylimidazole (phim). In both cases, the atomic coordinates of the molecules obtained in the crystal structures were used as the starting points and references for geometry optimisation. The calculated structural parameters related to the C–H···Ni interaction and the molecular conformations are listed in Table 2.

In the case of **1**, the overall conformation of the molecule in the optimised structure is comparable with that found in the solid-state X-ray structure. With regard to the molecular conformation the only major difference between the optimised and the experimental structures is in the dihedral angle between the phenyl ring plane and the plane containing the rest of the atoms of the bhac^{2-} ligand. In the optimised structure the whole tridentate ligand is essentially planar. It may be noted that the X-ray structure of **1** shows an intramolecular C–H $\cdots\pi$ interaction between the phenyl ring of bhac^{2-} and that of phim (vide supra). It is very likely that this interaction is responsible for the nonplanarity of bhac^{2-} in the experimental structure. For the present level of calculation we could not reproduce the C–H $\cdots\pi$ interaction in the optimised geometry. The calculated geometrical parameters indicate a more linear C–H $\cdots\text{Ni}$ interaction compared with that in the experimental structure (Table 2).

The same optimised molecular structure is obtained from the X-ray structural coordinates of the four molecules present in the asymmetric unit of **2**. The optimised molecule of **2** is very similar to that of **1** with regard to the Ni $\cdots\text{H}$ distance, C–H $\cdots\text{Ni}$ angle and ψ and θ values (Table 2). However, this optimised structure is rather different when compared with the structures of the four molecules obtained in the X-ray structure of **2**. In general, the twisting of phim (ψ) is much less, the imidazole ring plane and the plane containing the two chelate rings are more orthogonal (θ) and the Ni $\cdots\text{H}$ –C interaction is more linear in the experimental structures than those in the optimised structure (Table 2).

The dependence of the conformational energies of **1** and **2** on the twisting (ψ) of phim has been analysed by performing single point energy calculations by varying ψ from 0 to 90°. The experimental structures of **1** and molecule 1 of **2** are used for these calculations. The relative energies (ΔE) with respect to the lowest energy (at $\psi \approx 35^\circ$ for **1** and $\psi \approx 15^\circ$ for **2**) are plotted against the ψ values (Figure 5). For **1** it is a symmetric well-like plot. On the other hand, for **2** below 20° the change in energy is very low compared with that above 20°. The energy increases by only 0.20 kcal mol $^{-1}$ due to the gradual decrease of ψ from 20 to 0°. The small increase of energy indicates the absence of any significant steric or electronic constraint for the twisting of the phim in this range of ψ . For this reason, it is very likely that four molecules with ψ values in the range 1.6–21.6° have been found in the asymmetric unit of **2**.

The nature of the C–H $\cdots\text{Ni}$ interaction in **1** and **2** has been examined by several computational methods. In a three-centre four-electron C–H $\cdots\text{M}$ interaction, the interacting hydrogen atom should have a more positive charge compared with the other hydrogen atoms that are away from the metal centre. The natural population analysis^[28] shows that the charge on the *ortho*-hydrogen atom of the phim phenyl ring, which is at the apical site of the metal centre, is more positive (by +0.009e and +0.010e for **1** and **2**, respectively) compared with the charge on the other *ortho*-hydrogen atom of the same phenyl ring. The nickel(II) centre has an empty d orbital as well as a lone pair. Thus

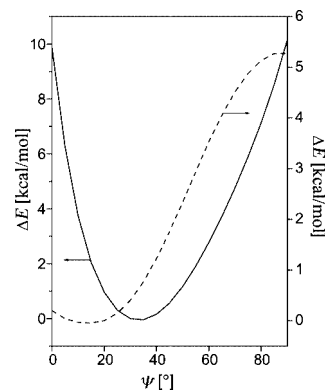


Figure 5. Relative energies of [Ni(bhac)(phim)] (**1**) (–) and [Ni(ahac)(phim)] (**2**) (---) as a function of twist angles (ψ) of 2-phenylimidazole (phim).

it can also accept electrons from the filled C–H σ orbital. The delocalisation energies for the C–H σ donation to the metal calculated through natural bond orbital analysis^[28] are 0.58 and 0.63 kcal mol $^{-1}$ for **1** and **2**, respectively. These delocalisation energies are insignificant compared with those obtained for strong agostic interactions and are comparable with C–H $\cdots\text{M}$ hydrogen-bonding interactions.^[29,30] The "atoms in molecules" theory^[31] has also been used for further probing of the topological properties of the C–H $\cdots\text{Ni}$ interaction in **1** and **2**. The values obtained for the electron densities ($\rho_b = 0.011$ and 0.012 a.u. for **1** and **2**, respectively) and the Laplacians ($\nabla^2\rho_b = 0.039$ and 0.041 a.u. for **1** and **2**, respectively) at the bond critical points are well within the range reported for C–H $\cdots\text{M}$ interactions that are hydrogen bonds in character.^[30,32–35]

Proton NMR Spectroscopic Studies

NMR spectroscopy is a useful tool for the diagnosis of the agostic or hydrogen-bond character of C–H $\cdots\text{M}$ interactions in square-planar d 8 metal ion complexes. The proton resonance shifts to an up-field position for agostic interactions while it shifts down-field for hydrogen-bond interactions compared with that of the free C–H group.^[9,11,36] The room temperature proton NMR spectra were recorded using $(\text{CD}_3)_2\text{CO}$ solutions of **1** and **2**. The protons of the two methyl groups of the acetylacetone fragment in **1** appear as two singlets at $\delta = 1.47$ and 2.20 ppm. The singlet observed at $\delta = 5.07$ ppm is assigned to the $-\text{CH}=\text{}$ group proton. The imidazole N–H proton resonates as a doublet at $\delta = 8.87$ ppm ($J = 8$ Hz). The multiplet observed in the range $\delta = 7.2$ –7.6 ppm is likely to be due to the imidazole ring C–H and aromatic protons. The absence of any cross-coupled peak in the 2D NMR spectrum of **1** indicates that the C–H $\cdots\pi$ interaction is probably absent in the solution state. In addition to all the above signals a broad singlet is observed at $\delta = 12.07$ ppm. This down-field signal is attributed to the *ortho*-C–H proton of the phim phenyl ring, which is proximal to the metal centre. It may be noted that the free phim or the Schiff bases do not show any resonance in this region. The protons of the three methyl groups of

ahac²⁻ in **2** are observed as three singlets at $\delta = 2.01$, 2.11 and 2.27 ppm. The proton of the –CH= group resonates as a singlet at $\delta = 5.51$ ppm. A broad singlet at $\delta = 8.89$ ppm is assigned to the imidazole N–H proton. As observed for **1** the signal from the phim phenyl ring *ortho* C–H proton, close to the apical site of the metal centre, appears down-field ($\delta = 11.63$ ppm) as a broad singlet. The multiplet in the range $\delta = 7.1$ –7.8 ppm corresponds to the imidazole ring C–H and the rest of the aromatic protons in the molecule.

We have recorded the NMR spectra of both complexes in the temperature range 20 to –80 °C and monitored the broad singlet observed at $\delta = 12.07$ and 11.63 ppm for **1** and **2**, respectively. In each case, the signal becomes sharper and is shifted further down-field on cooling (Figure 6). The shifts are 0.75 and 0.90 ppm for **1** and **2**, respectively. The observation of the down-field signal and its behaviour on lowering the temperature suggest that the C–H⋯Ni interaction present in the solid-state structures of both **1** and **2** is also present in solution and it is essentially hydrogen bond in character.

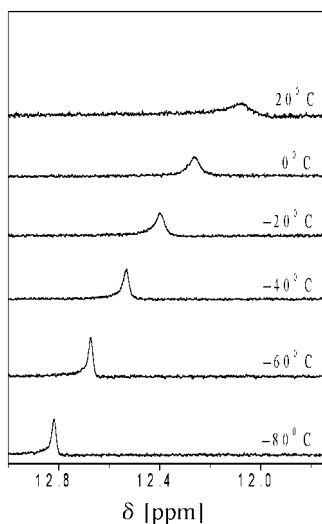


Figure 6. Temperature dependence of the down-field signal in the proton NMR spectrum of [Ni(bhac)(phim)] (**1**).

Conclusions

The tridentate O,N,O-donor benzoyl- and acetylhydrazone of acetylacetone (H₂bhac and H₂ahac) and monodentate N-donor 2-phenylimidazole (phim) yielded square-planar nickel(II) complexes [Ni(bhac)(phim)] (**1**) and [Ni(ahac)(phim)] (**2**). X-ray crystal structures reveal that the asymmetric unit of **1** contains a single molecule while that of **2** contains four molecules with different conformations. The conformation of **1** is significantly different compared with that of any of the four molecules of **2**. Perhaps the intramolecular C–H⋯ π interaction present in **1** is one of the factors for this difference. In each of **1** and **2**, one of the two *ortho* hydrogen atoms of the phim phenyl ring is very close to the metal centre at the apical site suggesting an intramolecular C–H⋯Ni interaction. The shape of the

C–H⋯Ni interaction depends on the twisting (ψ) of the phim and the extent of the orthogonality (θ) between the plane containing the chelate rings and the imidazole plane. The observed trends are compared with the structures of similar species reported in the literature. Theoretically optimised structures of both **1** and **2** are very similar. Energy calculations were performed by varying ψ from 0 to 90° for both **1** and **2**. The conformer of **1** having a ψ value of $\approx 35^\circ$ (experimental $\psi = 35.8^\circ$) is at the lowest energy and the plot of the relative energies (ΔE) of various conformers against ψ provides a reasonably symmetric well-type curve. For **2** the lowest energy conformer has a ψ value of $\approx 20^\circ$. However, the energy change is very little below $\psi = 20^\circ$. This observation explains the presence of four molecules having ψ in the range 1.6–21.6° in the asymmetric unit of **2**. Theoretical investigations suggest that a hydrogen-bond description of the C–H⋯Ni interaction in both **1** and **2** is more appropriate. In the NMR spectra of **1** and **2**, the appearance of this interacting proton at down-field and further down-field shifts, because of the lowering of the temperature, substantiates the hydrogen-bond character of this interaction.

Experimental Section

Materials: The Schiff bases H₂bhac and H₂ahac were prepared by condensation reactions of acetylacetone with benzoylhydrazine and acetylhydrazine, respectively.^[21] All other chemicals and solvents used in this work were of analytical grade, available commercially and were used without further purification.

Physical Measurements: Microanalytical (C, H, N) data were obtained with a Thermo Finnigan Flash EA1112 series elemental analyser. Infrared spectra were collected by using KBr pellets with a Jasco-5300 FT-IR spectrophotometer. A Shimadzu 3101-PC UV/Vis/NIR spectrophotometer was used to record the electronic spectra. The proton NMR spectra were recorded with a Bruker 400 MHz spectrometer. Solution electrical conductivities were measured with a Digisun DI-909 conductivity meter. A Sherwood Scientific balance was used for magnetic susceptibility measurements. A CH-Instruments model 620A electrochemical analyser was used for cyclic voltammetric experiments with acetonitrile solutions of the complexes containing tetrabutylammonium perchlorate (TBAP) as the supporting electrolyte. The three electrode measurements were carried out at 298 K under a dinitrogen atmosphere with a platinum disc working electrode, a platinum wire auxiliary electrode and an Ag/AgCl reference electrode.

Synthesis of the Complexes

[Ni(bhac)(phim)] (1**):** A dry methanol solution (15 cm³) of Ni(O₂CCH₃)₂·4H₂O (125 mg, 0.5 mmol) was added to a dry methanol solution (10 cm³) of H₂bhac (110 mg, 0.5 mmol) and 2-phenylimidazole (72 mg, 0.5 mmol). The resulting deep brown mixture was kept under reflux for 2 h and then evaporated on a steam bath to approximately half of the original volume. The brown needles that separated after cooling to room temperature were collected by filtration, washed with a little ice-cold methanol and finally dried in air. The yield obtained was 160 mg (76%). A single crystal suitable for X-ray structure determination was selected from this material. NiC₂₁H₂₀N₄O₂ (419.12): calcd. C 60.18, H 4.81, N 13.37; found C 59.95, H 4.78, N 13.24. Electronic spectroscopic data in CH₃OH:

λ_{max} (ϵ) = 565 sh (94), 380 (14200), 366 sh (12700), 267 (19800), 234 sh (21100) nm.

[Ni(ahac)(phim)] (2): A dry methanol solution (15 cm³) of Ni(O₂CCH₃)₂·4H₂O (125 mg, 0.5 mmol) was added to a dry methanol solution (10 cm³) of H₂ahac (70 mg, 0.5 mmol) and 2-phenylimidazole (72 mg, 0.5 mmol), and the mixture was kept under reflux for 2 h. A brown crystalline material was deposited on the wall of the round-bottomed flask along the surface of the solvent and formed a ring. The reaction mixture was cooled to room temperature and the almost colourless and clear mother liquor was removed carefully by using a dropper. The crystalline material was collected after drying in air. The yield obtained was 110 mg (62%). A single crystal suitable for X-ray structure determination was selected from this material. NiC₁₆H₁₈N₄O₂ (357.05): C 53.82, H 5.08, N 15.69; found C 53.54, H 4.86, N 15.47. Electronic spectroscopic data in CH₃OH: λ_{max} (ϵ) = 425 sh (370), 358 sh (3500), 344 (4700), 330 sh (4400), 267 (18400), 235 sh (18600) nm.

X-ray Crystallography: Complexes **1** and **2** crystallise in the space groups *C2/c* and *P2₁/c*, respectively. Unit cell parameters and the intensity data were obtained with a Bruker-Nonius SMART APEX CCD single-crystal diffractometer, equipped with a graphite monochromator and a Mo-*K_α* fine-focus sealed tube (λ = 0.71073 Å) operated at 2.0 kW. The detector was placed at a distance of 6.0 cm from the crystal. Data were collected at 298 K with a scan width of 0.3° in ω and an exposure time of 30 sec/frame. The SMART software was used for data acquisition and the SAINT-Plus software was used for data extraction.^[37] In each case, an absorption correction was performed with the help of the SADABS programme.^[38] The structures were solved by direct methods and refined on F^2 by full-matrix least-squares procedures. In both structures, all non-hydrogen atoms were refined with anisotropic thermal parameters. Hydrogen atoms were added at idealised positions by using a riding model. For **1** the hydrogen atoms were refined isotropically while for **2** they were not refined. The SHELX-97 programmes^[39] of the WinGX package^[40] were used for structure solution and refinement. The ORTEP6a^[41] and Platon^[42] packages were used for molecular graphics. Significant crystallographic data for **1** and **2** are summarised in Table 4.

Table 4. Selected crystallographic data for **1** and **2**.

| Complex | [Ni(bhac)(phim)] (1) | [Ni(ahac)(phim)] (2) |
|---|--|--|
| Empirical formula | C ₂₁ H ₂₀ N ₄ O ₂ Ni | C ₁₆ H ₁₈ N ₄ O ₂ Ni |
| Formula mass [g mol ⁻¹] | 419.12 | 357.05 |
| Crystal system | monoclinic | monoclinic |
| Space group | <i>C2/c</i> | <i>P2₁/c</i> |
| <i>a</i> [Å] | 43.532(3) | 24.450(2) |
| <i>b</i> [Å] | 11.8872(9) | 8.5337(7) |
| <i>c</i> [Å] | 7.6363(6) | 33.518(3) |
| β [°] | 99.3510(10) | 108.985(2) |
| <i>V</i> [Å ³] | 3899.1(5) | 6613.2(9) |
| <i>Z</i> | 8 | 16 |
| μ [mm ⁻¹] | 1.019 | 1.188 |
| Reflections collected | 19894 | 49271 |
| Reflections unique | 3853 | 8643 |
| Reflections [$I \geq 2\sigma(I)$] | 3013 | 4844 |
| Parameters | 333 | 841 |
| R_1, wR_2 [$I \geq 2\sigma(I)$] | 0.0361, 0.0889 | 0.0713, 0.1155 |
| R_1, wR_2 (all data) | 0.0488, 0.0970 | 0.1408, 0.1375 |
| GOF on F^2 | 0.913 | 1.025 |
| Largest peak, hole [e Å ⁻³] | 0.388, -0.201 | 0.400, -0.332 |

CCDC-294281 and CCDC-294282 contain the supplementary crystallographic data for **1** and **2**, respectively. These data can be

obtained free of charge from the Cambridge Crystallographic Data Centre via www.ccdc.cam.ac.uk/data_request/cif.

Computational Methods: DFT calculations for **1** and **2** were performed at the B3LYP/6-311G(d,p) level.^[43–45] The starting points of the geometry optimisations were the X-ray structural coordinates of the single molecule of **1** and of the four independent molecules of **2** found in the corresponding asymmetric units. The Gaussian 03^[46] suite of programmes was used for all calculations.

Supporting Information (see footnote on the first page of this article): Plots of C–H···Ni angles, ψ and θ (see text for definitions) against the Ni···H distances for **1** and **2** (Figure S1).

Acknowledgments

Financial support for this work was provided by the Council of Scientific and Industrial Research (CSIR) [Grant No. 01(1880)/03/EMR-II]. A. Mukhopadhyay thanks the CSIR for a research fellowship. We thank B. Pathak and T. S. Thakur for helpful discussions on the theoretical calculations. All calculations were done using the computational facility at the Centre for Modelling, Simulation and Design, University of Hyderabad. X-ray crystallographic studies were performed at the National Single Crystal Diffractometer Facility, School of Chemistry, University of Hyderabad (funded by the Department of Science and Technology). We thank the University Grants Commission for the facilities provided under the UPE and CAS programmes.

- [1] M. Brookhart, M. L. H. Green, *J. Organomet. Chem.* **1983**, 250, 395.
- [2] J.-Y. Saillard, R. J. Hoffman, *J. Am. Chem. Soc.* **1984**, 106, 2006.
- [3] M. Brookhart, M. L. H. Green, L. L. Wong, *Prog. Inorg. Chem.* **1988**, 36, 1.
- [4] R. H. Crabtree, D. G. Hamilton, *Adv. Organomet. Chem.* **1988**, 28, 299.
- [5] A. D. Ryabov, *Chem. Rev.* **1990**, 90, 403.
- [6] R. H. Crabtree, *Angew. Chem. Int. Ed. Engl.* **1993**, 32, 789.
- [7] A. J. Canty, G. van Koten, *Acc. Chem. Res.* **1995**, 28, 406.
- [8] D. Braga, F. Grepioni, E. Tedesco, K. Biradha, G. R. Desiraju, *Organometallics* **1997**, 16, 1846.
- [9] W. Yao, O. Eisenstein, R. H. Crabtree, *Inorg. Chim. Acta* **1997**, 254, 105.
- [10] T. W. Hambley, *Inorg. Chem.* **1998**, 37, 3767.
- [11] M. J. Calhorda, *Chem. Commun.* **2000**, 801.
- [12] L. Brammer, *Dalton Trans.* **2003**, 3145.
- [13] A. Albinati, P. S. Pregosin, F. Wombacher, *Inorg. Chem.* **1990**, 29, 1812.
- [14] M. Bortolin, U. E. Bucher, H. Rügger, L. M. Venanzi, A. Albinati, F. Lianza, S. Trofimenko, *Organometallics* **1992**, 11, 2514.
- [15] T. Hascall, M.-H. Baik, B. M. Bridgewater, J. H. Shin, D. G. Churchill, R. A. Friesner, G. Parkin, *Chem. Commun.* **2002**, 2644.
- [16] W. Kemp, *Organic Spectroscopy*, Macmillan, Hampshire, **1987**, pp. 62–66.
- [17] K. Nakamoto, *Infrared and Raman Spectra of Inorganic and Coordination Compounds*, Wiley, New York, **1986**, pp. 241–242.
- [18] S. Das, S. Pal, *J. Organomet. Chem.* **2004**, 689, 352.
- [19] S. G. Sreerama, S. Pal, *Inorg. Chem.* **2005**, 44, 6299.
- [20] S. G. Sreerama, S. Pal, *Eur. J. Inorg. Chem.* **2004**, 4718.
- [21] N. R. Sangeetha, C. K. Pal, P. Ghosh, S. Pal, *J. Chem. Soc., Dalton Trans.* **1996**, 3293.
- [22] S. Das, G. P. Muthukumaragopal, S. N. Pal, S. Pal, *New J. Chem.* **2003**, 27, 1102.
- [23] S. Das, S. Pal, *J. Mol. Struct.* **2005**, 741, 183.

- [24] A. Mukhopadhyay, G. Padmaja, S. N. Pal, S. Pal, *Inorg. Chem. Commun.* **2003**, 6, 381.
- [25] A. Mukhopadhyay, S. Pal, *Polyhedron* **2004**, 23, 1997.
- [26] G. V. Karunakar, N. R. Sangeetha, V. Susila, S. Pal, *J. Coord. Chem.* **2000**, 50, 51.
- [27] D. R. Trivedi, A. Ballabh, P. Dastidar, *CrystEngComm* **2003**, 5, 358.
- [28] A. E. Reed, L. A. Curtiss, F. Weinhold, *Chem. Rev.* **1988**, 88, 899.
- [29] R. B. Cracknell, A. G. Orpen, J. L. Spencer, *J. Chem. Soc., Chem. Commun.* **1984**, 326.
- [30] T. S. Thakur, G. R. Desiraju, *Chem. Commun.* **2006**, 552.
- [31] R. F. W. Bader, *Atom in Molecules, A Quantum Theory*, The Clarendon Press, Oxford, **1990**.
- [32] U. Koch, P. L. A. Popelier, *J. Phys. Chem.* **1995**, 99, 9747.
- [33] P. L. A. Popelier, G. Logothetis, *J. Organomet. Chem.* **1998**, 555, 101.
- [34] S. Pillet, G. Wu, V. Kulsomphob, B. G. Harvey, R. D. Ernst, P. Coppens, *J. Am. Chem. Soc.* **2003**, 125, 1937.
- [35] C.-S. Liu, P.-Q. Chen, E.-C. Yang, J.-L. Tian, X.-H. Bu, Z.-M. Li, H.-W. Sun, Z. Lin, *Inorg. Chem.* **2006**, ASAP article.
- [36] A. J. Canty, G. van Koten, *Acc. Chem. Res.* **1995**, 28, 406.
- [37] *SMART V5.630 and SAINT-plus V6.45*, Bruker-Nonius Analytical X-ray Systems Inc., Madison, WI, USA, **2003**.
- [38] G. M. Sheldrick, *SADABS Program for area detector absorption correction*, University of Göttingen, Göttingen, Germany, **1997**.
- [39] G. M. Sheldrick, *SHELX-97 Structure Determination Software*, University of Göttingen, Göttingen, Germany, **1997**.
- [40] L. J. Farrugia, *J. Appl. Crystallogr.* **1999**, 32, 837.
- [41] P. McArdle, *J. Appl. Crystallogr.* **1995**, 28, 65.
- [42] A. L. Spek, *PLATON A Multipurpose Crystallographic Tool*, Utrecht University, Utrecht, The Netherlands, **2002**.
- [43] A. D. Becke, *J. Chem. Phys.* **1993**, 98, 5648.
- [44] C. Lee, W. Yang, R. G. Parr, *Phys. Rev. B* **1988**, 37, 785.
- [45] T. H. Dunning Jr, P. J. Hay, *Modern Theoretical Chemistry* (Ed.: H. F. Schaefer III), Plenum, New York, **1976**, pp. 1–28.
- [46] M. J. Frisch et al., *Gaussian 03 Revision B05*, Gaussian Inc., Pittsburgh, PA, **2004**.

Received: June 24, 2006

Published Online: October 10, 2006